

# Octanoate oxidation measured by $^{13}\text{C}$ -NMR spectroscopy in rat skeletal muscle, heart, and liver

Marlei E. Walton,<sup>1</sup> Douglas Ebert,<sup>1</sup> and Ronald G. Haller<sup>1,2,3</sup>

<sup>1</sup>Department of Veterans Affairs North Texas Health Care System, Dallas 75216; <sup>2</sup>Department of Neurology, University of Texas Southwestern Medical Center, Dallas 75235; and <sup>3</sup>Institute for Exercise and Environmental Medicine, Presbyterian Hospital of Dallas, Dallas, Texas 75231

Submitted 2 October 2002; accepted in final form 22 July 2003

**Walton, Marlei E., Douglas Ebert, and Ronald G. Haller.** Octanoate oxidation measured by  $^{13}\text{C}$ -NMR spectroscopy in rat skeletal muscle, heart, and liver. *J Appl Physiol* 95: 1908–1916, 2003. First published July 25, 2003; 10.1152/jappphysiol.00909.2002.—Contribution of octanoate to the oxidative metabolism of the major sites of fatty acid oxidation (heart, liver, and resting and contracting skeletal muscle) was assessed in the intact rat with  $^{13}\text{C}$ -NMR spectroscopy. Under inhalation anesthesia, [2,4,6,8- $^{13}\text{C}_4$ ]octanoate was infused into the jugular vein and the sciatic nerve of one limb was stimulated for 1 h. Octanoate was a principal contributor to the acetyl-CoA pool in all tissues examined, with highest oxidation occurring in heart and soleus muscle followed by predominantly red portion of gastrocnemius muscle (RG), liver, and then white portion of gastrocnemius muscle (WG). Fractional contribution of  $^{13}\text{C}$ -labeled octanoate to the acetyl-CoA pool (Fc2) was  $0.563 \pm 0.066$  for heart and  $0.367 \pm 0.054$  for liver. Significant differences were observed between each of the muscle types during both rest and contraction. In muscle, Fc2 was highest in soleus ( $0.565 \pm 0.089$  rested,  $0.564 \pm 0.096$  contracted), followed by RG ( $0.470 \pm 0.092$  rested,  $0.438 \pm 0.072$  contracted), and lowest in WG ( $0.340 \pm 0.081$  rested,  $0.272 \pm 0.065$  contracted). Our findings demonstrate that the fractional contribution of octanoate to oxidative metabolism correlates with oxidative capacity of the tissue and that octanoate metabolism increases in contracted muscle in proportion to the overall increase in oxidative rate.

$^{13}\text{C}$  isotopomer analysis; metabolism; nuclear magnetic resonance; fiber type

ADMINISTRATION OF OCTANOATE has been used to examine medium-chain fatty acid metabolism in both human and animal studies. In particular, it has been used in humans to study the relationship between carbohydrate and fat metabolism during exercise (3, 5, 13, 32, 33). Additionally, octanoate is a prominent component of the medium-chain triglycerides (MCT) found in pre-term infant formulas, accounting (with decanoate) for up to 85% of total fat oxidation (34). MCT oil is also used clinically in the treatment of inborn errors of metabolism (10, 30). Although octanoate contribution to overall oxidation can be assessed with tracer analysis, the relative extent to which octanoate supplies

oxidative energy requirements in different tissues in these subjects is not well understood (2).

The fate of octanoate in the whole animal is complex. To date, no study has concomitantly examined octanoate oxidation in all of the primary sites of fatty acid oxidation, namely, heart, skeletal muscle, and liver (27). Octanoate metabolism has been studied in heart (8), skeletal muscle (38), and liver (24), but all of these studies have been in isolated tissue.  $^{13}\text{C}$  magnetic resonance spectroscopy (MRS) analysis methodology allows simultaneous examination of octanoate oxidation in multiple tissues and furnishes information about the metabolic conversion of  $^{13}\text{C}$ -labeled octanoate to other labeled substrates to more completely assess the metabolic fate of octanoate in the whole animal. Octanoate oxidation has been studied in the intact rat (9, 14). However, these studies did not include all of the primary sites of fatty acid oxidation (9, 14) and the latter study examined a combination of exogenous substrates (14).

Results from combined studies demonstrated that more oxidative tissue has the potential to utilize fats to a greater degree than less oxidative tissue (9, 36, 37). However, the degree to which this occurs in the major fatty acid-utilizing tissues of an intact animal is not known. In light of previous data and intrinsic properties such as mitochondrial density, presence of oxidative enzymes, and capillary density, we hypothesized that fatty acid contribution to oxidation would be greatest in heart, followed by oxidative muscle and liver, and least in glycolytic muscle. To support oxygen consumption increases during contraction, muscle increases utilization of both plasma free fatty acids and triglyceride fat sources (37). We postulated that octanoate utilization would increase with contraction and be reflected in a similar or higher fractional contribution of  $^{13}\text{C}$ -labeled octanoate to oxidative metabolism in contracted vs. resting muscles.

## MATERIALS AND METHODS

[2,4,6,8- $^{13}\text{C}_4$ ]octanoate was infused into the jugular vein of an intact rat over the course of 1 h, and the contribution of octanoate to the oxidative metabolism of heart, liver, and

Address for reprint requests and other correspondence: M. E. Walton, Veterans Affairs North Texas Health Care System, 4500 South Lancaster Road (151), Dallas, TX 75216 (E-mail: mwde@swbell.net).

The costs of publication of this article were defrayed in part by the payment of page charges. The article must therefore be hereby marked "advertisement" in accordance with 18 U.S.C. Section 1734 solely to indicate this fact.

rested and contracted gastrocnemius and soleus muscle was determined. Blood and plasma samples were analyzed to quantitate levels of  $^{13}\text{C}$ octanoate, metabolite concentrations, as well as the conversion of  $^{13}\text{C}$ octanoate into other labeled substrates.

**Animal preparation.** All experimental procedures were approved by the Institutional Animal Care and Use Committee at the Department of Veterans Affairs North Texas Health Care System (VANTHCS) and the Institutional Animal Care and Research Advisory Committee at the University of Texas Southwestern Medical Center. Male Sprague-Dawley rats ( $346.4 \pm 19.5$  g; Charles River, Kingston, MA) were housed in the VANTHCS Animal Resources Center with a 12:12-h light-dark cycle and ad libitum access to water and lab chow.

Rats were weighed and anesthetized with an intraperitoneal injection of 1–3 ml/kg ketamine-xylazine mixture (6 mg/ml xylazine, 94 mg/ml ketamine). After a tracheotomy was performed, 1–2.5% isoflurane (Isotec 3 vaporizer; Matrix Medical, Buffalo, NY) in a 100%  $\text{O}_2$  mixture was used to maintain anesthesia and was delivered via a positive-pressure ventilator (model 683 small animal ventilator; Harvard Apparatus, South Natick, MA) at a rate of 1.25 ml/min,  $\sim 100$  breaths/min. The right carotid artery was catheterized and connected to a fluid-filled pressure transducer (model P23XL Gould Transducer; Future Tech, Birmingham, AL) to continuously monitor heart rate and blood pressure throughout the surgical procedure. Systemic arterial blood gases were monitored with a blood gas analyzer (ABL-4, Radiometer, Westlake, OH). The gas mixture and/or ventilation rate was adjusted to maintain blood pH of 7.3–7.4 and arterial  $\text{O}_2$  saturation of 99+%. After arterial cannulation, the jugular vein was cannulated and connected to an infusion pump (model 22, Harvard Apparatus) for the administration of labeled and unlabeled octanoate. Initially, unlabeled 220 mM sodium octanoate (Aldrich, Milwaukee, WI) was infused at a rate of 2.67 ml/h. Temperature was maintained at 37°C with an external heating pad placed under the rat, in combination with the heat radiating from the incandescent light source illuminating the surgical field. Both calcaneal tendons and the left sciatic nerve pocket were surgically isolated. The left sciatic nerve was bathed in mineral oil and isolated from surrounding tissue. Nerve viability was maintained by regular topical application of mineral oil during the remainder of the experiment.

**Experimental design.** At time zero, after  $\sim 30$  min of unlabeled octanoate infusion, the infusate was changed to 220 mM sodium [2,4,6,8- $^{13}\text{C}_4$ ]octanoate [Cambridge Isotope Laboratories (CIL), Andover, MA] and the muscles of the left limb were contracted via direct electrical stimulation to the sciatic nerve. Custom-built silver electrodes connected to an electrical stimulator and isolation unit (Grass models S88 and S7; New Astromed, West Warwick, RI) were used to deliver 100-ms trains of pulses (100 Hz, 0.2-ms duration, no delay) at the voltage required to elicit maximal force output (typically 3.5–5 V) at 0.5 Hz for 60 min. The left calcaneal tendon was attached to a force transducer (Grass model FT-10; New Astromed), and the output was recorded with PolyVIEW software (Grass; New Astromed). Force drop-off to  $76 \pm 12\%$  of the original value occurred by the end of the experiment. Once the experiment was completed, gastrocnemius and soleus muscles were isolated from the contracted hindlimb and then from the contralateral unstimulated (rested) hindlimb, followed by isolation of the liver and heart. Isolated tissue was immediately frozen in liquid nitrogen and stored at  $-80^\circ\text{C}$  until extraction.

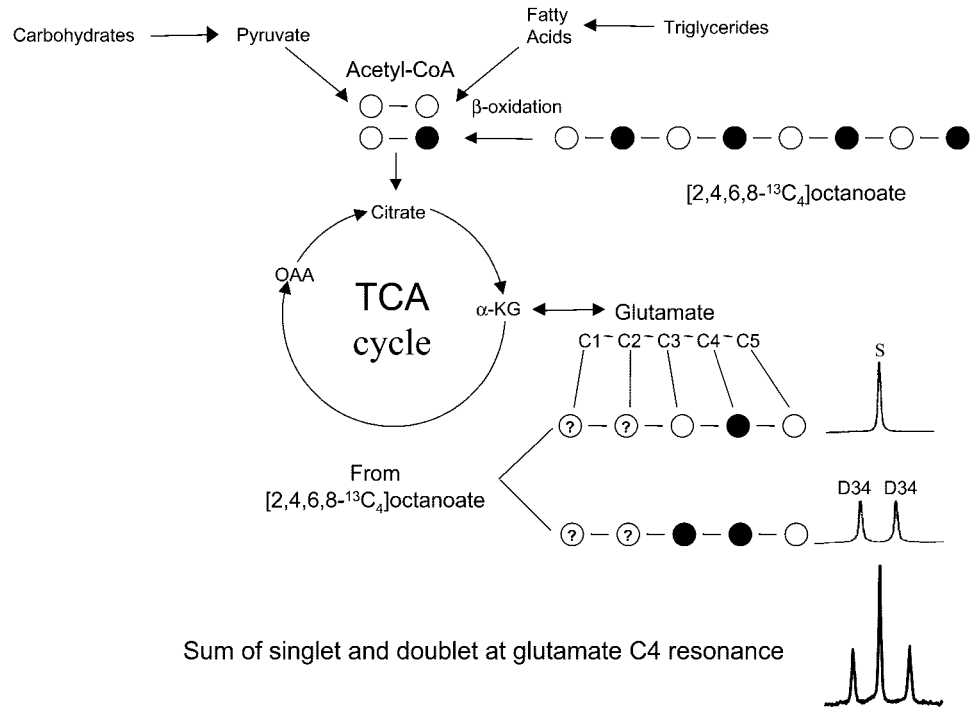
**Plasma metabolite concentration.** Arterial blood (410  $\mu\text{l}$ ) taken from the carotid artery was obtained 1) before any octanoate infusion (endogenous), 2) after the infusion of unlabeled octanoate but before infusion of  $^{13}\text{C}$ -labeled octanoate (0 min), and 3) at the end of the experiment (60 min); 370  $\mu\text{l}$  was centrifuged; and the plasma was analyzed to determine the enrichment and concentration of octanoate with GC-MS (26), insulin (rat insulin RIA kit, Linco Research, St. Charles, MO), and free fatty acids (NEFA kit, Wako Chemical, Richmond, VA) at these time points. Octanoate was assayed by derivatization with 2,4-difluoroaniline, with 1,3-dicyclohexylcarbodiimide as a coupling agent. [9,9,9- $^2\text{H}_3$ ]nonanoate was used as an internal standard. Forty-microliter blood aliquots were immediately mixed with 400  $\mu\text{l}$  of ice-cold 4% perchloric acid (PCA) and used subsequently to measure glucose, lactate, pyruvate, and ketones (acetoacetate and  $\beta$ -hydroxybutyrate) fluorometrically (23).

**Tissue preparation.** Immediately before extraction, gastrocnemius muscles were immersed in ice-cold saline and separated into white (primarily type IIb muscle fibers; Ref. 7) and predominantly red (mostly type IIa muscle fibers; Ref. 7) components. Isolated soleus (mainly type I muscle fibers; Ref. 7) and gastrocnemius muscle, heart, and liver were homogenized in ice-cold 3.6% PCA with a motor-driven tissue grinder (model 985–370; Biospec Products, Bartlesville, OK). Tissue homogenates and PCA-extracted blood samples were spun for 15 min at 20,000  $g$ . The supernatant was then neutralized, spun for 15 min at 20,000  $g$ , and lyophilized overnight in a rotary evaporator (Speedvac, Savant Instruments, Farmingdale, NY; Flexi-Dry microprocessor lyophilizer, FTS Systems, Stone Ridge, NY). The lyophilate was then brought to a volume of  $\sim 550$   $\mu\text{l}$  in deuterium oxide (99.8% enrichment; CIL).

**NMR methods.** Proton-decoupled  $^{13}\text{C}$ - and solvent-suppressed  $^1\text{H}$ -NMR spectra of the tissue extracts were collected at 37°C on a Varian INOVA 600-MHz spectrometer (Varian, Palo Alto, CA) in a 5-mm broad-band probe.  $^{13}\text{C}$ -NMR spectra were obtained with 300-KHz sweep width, 45° pulse, 1.5-s pulse delay, and bilevel proton decoupling. To achieve adequate signal to noise, the number of scans acquired was typically 100 for heart, 1K for liver and blood, 8K for the predominantly red portion of the gastrocnemius muscle, 10K for soleus muscle, and 12K for the white portion of the gastrocnemius muscle. Solvent-suppressed  $^1\text{H}$  spectra were collected with pulse width of 9.2  $\mu\text{s}$ , 10-s pulse delay, and 32 scans/sample. Free induction decays were baseline corrected and multiplied by an exponential function before Fourier transformation; 0.5-Hz line broadening was used for all extracts. The areas and intensities of  $^{13}\text{C}$  and  $^1\text{H}$  spectra were quantitated by a curve-fitting program (NUTS, Acorn, Fremont, CA). The line fit was considered adequate if the difference spectra were indistinguishable from spectral regions with no visible peaks. For  $^{13}\text{C}$ glutamate regions, each multiplet area was normalized and reported as a fraction of the total area for that specific carbon resonance.

Non-steady-state isotopomer analysis (Fig. 1) was used to calculate fractional enrichment values and assess the oxidation of the [2,4,6,8- $^{13}\text{C}_4$ ]octanoate and unlabeled substrates to the acetyl-CoA pool (21). This methodology is quite robust and takes advantage of two important chemical properties: 1) chemical shift, which permits each glutamate carbon to be resolved separately from the carbons of other metabolites in the  $^{13}\text{C}$  spectrum; and 2) carbon-carbon coupling, which gives information about neighboring labeled carbons, indicating how the labeled substrate has been incorporated into the tissue and utilized. By using the relative intensities of multiplets arising from a single glutamate carbon resonance as

Fig. 1.  $^{13}\text{C}$  isotope isomer (isotopomer) analysis is based on the appearance of  $^{13}\text{C}$  label (●) from  $[2,4,6,8-^{13}\text{C}_4]$ octanoate in the carbons of glutamate. Glutamate is in rapid exchange with the TCA cycle intermediate  $\alpha$ -ketoglutarate ( $\alpha$ -KG) and is present in concentrations high enough to be readily detected with magnetic resonance spectroscopy. Label entering the TCA cycle for the first time gives rise to a single peak (singlet, S) in the glutamate carbon 4 (C-4) region. As the TCA cycle turns over,  $^{13}\text{C}$  label is mixed at symmetrical intermediates, giving rise to label in adjacent carbons, which splits those carbons' signals into multiple peaks (multiplets). For example, if C-2-labeled oxaloacetate condenses with methyl-labeled acetyl-CoA (from exogenous octanoate), a doublet (D34) will be seen [due to carbon-carbon coupling (J) 34] in the area where glutamate C-4 resonates in the  $^{13}\text{C}$  spectrum as shown. The combination of the singlet and D34 in the glutamate C-4 region will be 3 peaks. This analysis can be done with other carbons of glutamate (e.g., C-3) or other metabolites (e.g., glucose). OAA, oxaloacetate.



well as the relative peak intensities of different carbons within glutamate, the fractional contribution of the starting labeled substrate to the acetyl-CoA pool can be determined. In these experiments, metabolism of the exogenously administered  $[2,4,6,8-^{13}\text{C}_4]$ octanoate is such that only carbon 2 (C-2) of the acetyl-CoA pool is labeled. The fractional contribution of this singly labeled acetyl-CoA (in C-2) to the entire acetyl-CoA pool is designated Fc2. We calculated Fc2 with the following equation:  $\text{Fc2} = (\text{C-4/C-3})(\text{C-4D34})$  (21), where C-4/C-3 represents the ratio of the area under all of the peaks in the glutamate carbon 4 region vs. those of the glutamate carbon 3 resonance and C-4D34 refers to the fractional contribution of the doublet arising from carbon-carbon coupling in C-3 and C-4 of glutamate to the entire peak area of the glutamate C-4 region. Contribution of natural-abundance  $^{13}\text{C}$  to the glutamate C-3 and C-4 singlets was accounted for by using endogenous taurine in the following manner. Ratios of the peak areas of glutamate C-3 and C-4 singlets to that of taurine C-2 were obtained in MRS experiments using only unlabeled octanoate. These ratios were then multiplied by the peak area of taurine C-2 in the  $^{13}\text{C}$  spectra of each tissue to calculate the glutamate C-3 and C-4 natural-abundance  $^{13}\text{C}$  peak areas, which were subtracted from their respective singlets in the  $^{13}\text{C}$  spectra of each tissue. The contribution to the acetyl-CoA pool from endogenous unlabeled sources (Fc0) was calculated with the equation  $\text{Fc0} = 1 - \text{Fc2}$  (21).

**Statistics.** Results are reported as means  $\pm$  SD. Student's *t*-test was used to compare all measured data. Paired two-tailed *t*-tests were used to make comparisons across one leg (different muscle fiber types of the same condition, i.e., either rested or contracted) or across one animal (rested vs. contracted muscle of the same fiber type). Unpaired two-tailed *t*-tests were used to make comparisons between different tissues or different time points;  $n = 5$  for each data point, except octanoate concentration for the 0 time point, where  $n = 4$  because of technical difficulties with one of the samples. Differences were considered significant when  $P \leq 0.05$ .

## RESULTS

**Fractional contribution of  $[2,4,6,8-^{13}\text{C}_4]$ octanoate.** Representative  $^{13}\text{C}$  spectra of extracts of rested (non-contracted) gastrocnemius and soleus muscle and of heart and liver infused in vivo with  $[2,4,6,8-^{13}\text{C}_4]$ octanoate for 60 min are shown in Fig. 2. Glutamate C-3 and C-4 regions are shown in each panel of Fig. 2; corresponding glutamate multiplet areas are listed in Table 1. As can be seen,  $^{13}\text{C}$  label from metabolism of the administered  $[2,4,6,8-^{13}\text{C}_4]$ octanoate was avidly incorporated into all of these tissues.

Non-steady-state isotopomer analysis (Table 2) indicated that the contribution of  $^{13}\text{C}$ -labeled octanoate to the acetyl-CoA pool was highest in soleus and heart, followed by the predominantly red portion of gastrocnemius, with lower levels in liver and in the white portion of gastrocnemius. The fractional contribution of  $[2,4,6,8-^{13}\text{C}_4]$ octanoate to the acetyl-CoA pool was 0.57 in rested soleus, indicating that 57% of acetyl CoA in this tissue was derived from labeled octanoate. In predominantly red gastrocnemius muscle (mostly type IIa muscle fibers), labeled acetyl-CoA from metabolism of  $[^{13}\text{C}]$ octanoate (Fc2) was  $>15\%$  lower at 0.47. In white gastrocnemius (primarily low-oxidative, high-glycolytic type IIb fibers), label incorporation resulting in glutamate multiplets was lower compared with those in the mainly red gastrocnemius and soleus muscles (Table 1) and the fractional contribution from  $^{13}\text{C}$ -labeled octanoate to the acetyl-CoA pool in the white portion of gastrocnemius was 0.34 (Table 2). The labeling pattern in the glutamate C-3 area of the  $^{13}\text{C}$  spectra differed among muscles, with a higher proportion of label in the C-3 doublet compared with the C-3

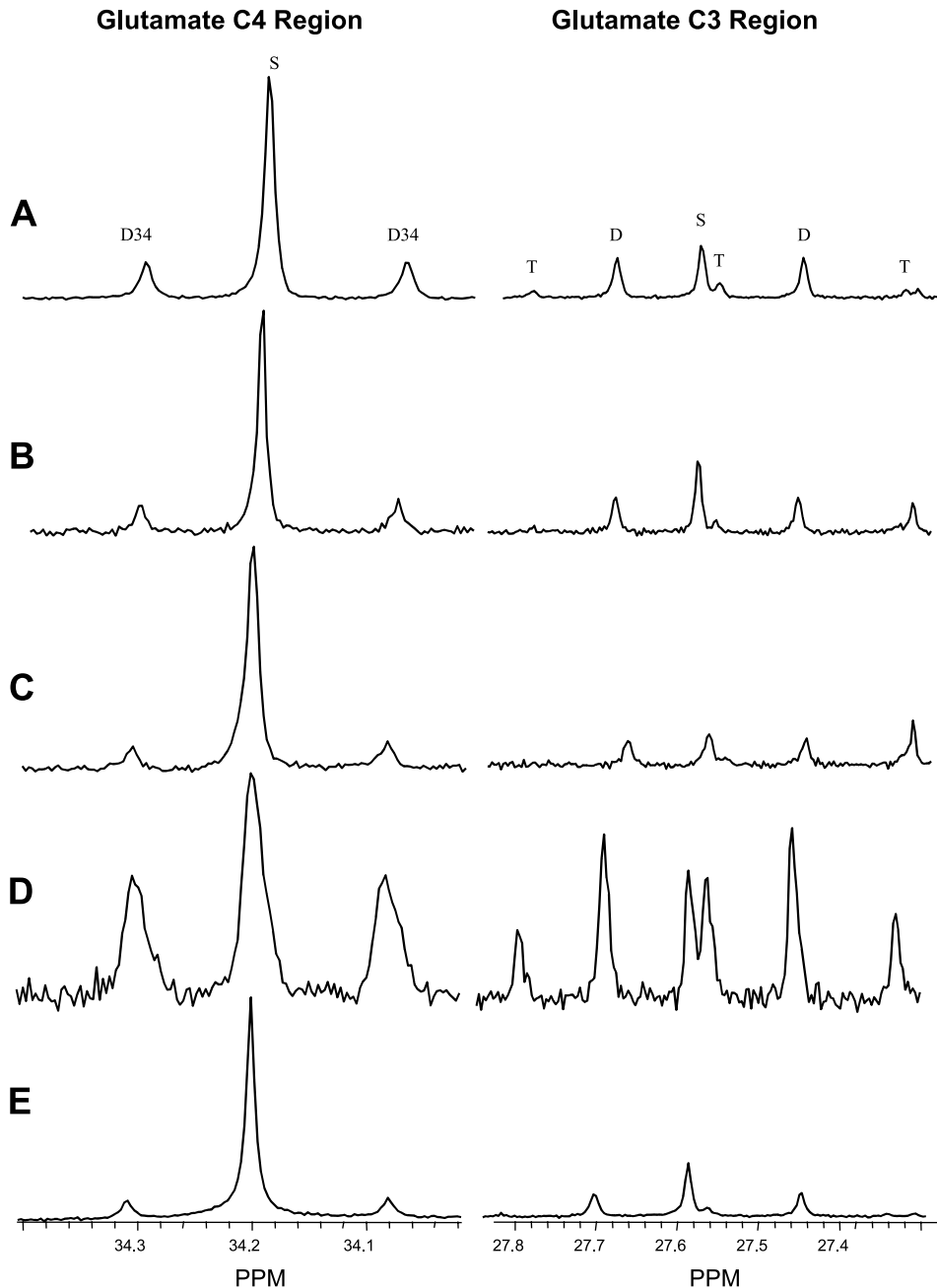


Fig. 2. Glutamate C-4 (left) and C-3 (right) regions are shown from <sup>13</sup>C spectra of representative extracts of rested predominantly red gastrocnemius muscle (IIa; A), white gastrocnemius muscle (IIb; B), soleus muscle (I; C), heart (D), and liver (E). The C-4 singlet (S) and doublet 34 (D34) are seen in the glutamate C-4 area, and the S, D, and triplet (T) are visible in the glutamate C-3 region. The doublet in glutamate C-3 (D) is not denoted with a specific carbon coupling because spin-spin coupling between C-2-C-3 and C-3-C-4 are equivalent. The glutamate C-3 triplet (T) is actually a doublet of doublets originating from <sup>13</sup>C labeling in the C-2, C-3, and C-4; however, the 2 inner resonance peaks overlap to produce a 1:2:1 peak “triplet” resonance.

singlet in soleus vs. predominantly red gastrocnemius and particularly white gastrocnemius (Table 1). This correlates with incorporation of label into the TCA cycle from [<sup>13</sup>C]octanoate oxidation; higher Fc2 and oxidative capacity increase the probability that labeled oxaloacetate will condense with labeled acetyl-CoA, which gives rise to the doublet 34 observed in the glutamate C-4 region and contributes to the doublet in the glutamate C-3 region.

Heart spectra show increased <sup>13</sup>C label incorporation in both the C-3 and C-4 multiplets of glutamate compared with skeletal muscle or liver (Fig. 2, Table 1), although the fractional contribution of <sup>13</sup>C-labeled octanoate to the acetyl-CoA pool (0.56) was virtually identical to that in soleus. The difference in labeling

pattern in heart reflects a greater level of incorporation in all C-4 and C-3 peaks relative to each other and a larger proportion of label in the doublet 34 relative to the singlet of C-4 and in both the doublet and triplet in the C-3 region relative to the singlet. This suggests higher TCA cycle turnover or lower flux of unlabeled substrates through anaplerotic pathways (or both) occurring in heart vs. the other tissues examined.

*Octanoate metabolism during muscle contraction.* <sup>13</sup>C spectra of extracts of contracted gastrocnemius and soleus muscle infused with [2,4,6,8-<sup>13</sup>C<sub>4</sub>]octanoate for 60 min were comparable to those of rested muscle (data not shown). As can be seen from Table 1, the <sup>13</sup>C label incorporation was quite similar during rest and contraction. Although the ratio of the area under the

Table 1. Glutamate multiplet areas in <sup>13</sup>C NMR spectra of muscle, heart, and liver extracts

	Rested	Contracted
<i>Gastrocnemius red (IIa)</i>		
C4D34	0.245 ± 0.042 <sup>b,d,e</sup>	0.258 ± 0.029 <sup>b,c</sup>
C3D	0.467 ± 0.039 <sup>b,c</sup>	<b>0.446 ± 0.032<sup>b</sup></b>
C3T	0.120 ± 0.033 <sup>b,d</sup>	0.137 ± 0.014
C4/C3	1.914 ± 0.147 <sup>c,d</sup>	1.695 ± 0.163 <sup>b,c</sup>
<i>Gastrocnemius white (IIb)</i>		
C4D34	0.187 ± 0.054 <sup>a,d</sup>	0.186 ± 0.043 <sup>a</sup>
C3D	0.369 ± 0.069 <sup>a,c,d</sup>	0.360 ± 0.046 <sup>a,c</sup>
C3T	0.079 ± 0.034 <sup>a,d</sup>	0.088 ± 0.048
C4/C3	1.832 ± 0.140 <sup>c,d</sup>	<b>1.469 ± 0.179<sup>a,c</sup></b>
<i>Soleus (I)</i>		
C4D34	0.193 ± 0.029 <sup>d</sup>	0.196 ± 0.022 <sup>a</sup>
C3D	0.522 ± 0.038 <sup>a,b,e</sup>	0.490 ± 0.093 <sup>b</sup>
C3T	0.094 ± 0.028 <sup>d</sup>	0.103 ± 0.038
C4/C3	2.979 ± 0.596 <sup>a,b,d,e</sup>	2.937 ± 0.727 <sup>a,b</sup>
<i>Heart</i>		
C4D34	0.463 ± 0.071 <sup>a,b,c,e</sup>	
C3D	0.488 ± 0.018 <sup>b,e</sup>	
C3T	0.264 ± 0.100 <sup>a,b,c,e</sup>	
C4/C3	1.224 ± 0.082 <sup>a,b,c,e</sup>	
<i>Liver</i>		
C4D34	0.183 ± 0.018 <sup>a,d</sup>	
C3D	0.412 ± 0.038 <sup>c,d</sup>	
C3T	0.122 ± 0.033 <sup>d</sup>	
C4/C3	2.014 ± 0.258 <sup>c,d</sup>	

Results are means ± SD (*n* = 5). C4 and C3 refer to carbon multiplets observed in enriched glutamate regions of the <sup>13</sup>C spectra. Each resonance is comprised of multiplets, denoted as doublet (D) and triplet (T) (singlet not shown). Each multiplet area is shown as a fraction of the total area for that specific carbon resonance. C4/C3 denotes the ratio of total peak areas in the C4 region to total peak areas in the C3 region. Values in bold are significantly (*P* < 0.05) different from rest. <sup>a</sup>Significantly different from predominantly red gastrocnemius muscle in same condition (rested vs. contracted), <sup>b</sup>significantly different from white gastrocnemius muscle in same condition, <sup>c</sup>significantly different from soleus muscle in same condition (heart and liver were compared with rested muscle), <sup>d</sup>significantly different from heart, <sup>e</sup>significantly different from liver (all *P* ≤ 0.05).

glutamate C-4 peaks vs. the area under the glutamate C-3 peaks is lower in contracted vs. rested white gastrocnemius muscle (Table 1), there are no statistical differences between rest and contraction in the fractional contribution of <sup>13</sup>C-labeled octanoate to the oxidative metabolism of either gastrocnemius or soleus muscles (Table 2).

Non-steady-state isotopomer analysis indicated that differences in the contribution of metabolized <sup>13</sup>C-labeled octanoate to the acetyl-CoA pool were similar to those found in rested muscle, with highest levels in soleus muscle, less in predominantly red gastrocnemius muscle, and least in white gastrocnemius muscle (Table 2). Label incorporation resulting in glutamate multiplets follows this same pattern (Table 1): incorporation is highest in the oxidative muscle and lowest in the glycolytic muscle.

**Blood and plasma metabolites.** Representative <sup>13</sup>C and <sup>1</sup>H spectra of blood extracts taken at the end of the experiments are shown in Fig. 3. As can be seen in the

<sup>13</sup>C spectrum (Fig. 3A), peaks are only visible in the regions where carbons from glucose, [2,4,6,8-<sup>13</sup>C<sub>4</sub>]octanoate, and β-hydroxybutyrate resonate. Examination of <sup>1</sup>H spectral data (Fig. 3B) reveals that glucose C-1α (5.24 ppm) is enriched slightly above the 1.1% natural abundance levels to 3.35 ± 0.79% and β-hydroxybutyrate C-4 (1.19 ppm) is enriched to 13.5 ± 10.5%. Plasma glucose levels increased slightly at the end of the experiment (12.9 mM) from the starting endogenous concentration (11.4 mM), and, although there was a rising trend in mean plasma insulin levels, statistical significance was not reached (Table 3). Ketones (β-hydroxybutyrate + acetoacetate) and lactate rose from their initial value on infusion of octanoate, but there was no difference in ketone or lactate concentration after ~30 min of unlabeled octanoate infusion vs. the end of the experiment (Table 3). Pyruvate did not change from endogenous values during the course of the experiment (Table 3). Plasma free fatty acids rose from their initial value on infusion of octanoate, but there was no difference in free fatty acid concentration after ~30 min of unlabeled octanoate infusion vs. the end of the experiment (Table 3). Likewise, octanoate concentration rose from initial nondetectable levels, but there was no difference in octanoate concentration after ~30 min of unlabeled octanoate infusion vs. the end of the experiment (Table 3). Labeled octanoate was not detected either in the initial measurements or in measurements made after ~30 min of unlabeled octanoate infusion. No unlabeled octanoate was detected with GC-MS in plasma at the end

Table 2. Non-steady-state <sup>13</sup>C analysis after 60-min infusion of [2,4,6,8-<sup>13</sup>C<sub>4</sub>]octanoate

Sources of Acetyl-CoA	Rested	Contracted
<i>Gastrocnemius red (IIa)</i>		
Fc2	0.470 ± 0.092 <sup>b,c</sup>	0.438 ± 0.072 <sup>b,c</sup>
Fc0	0.530 ± 0.092 <sup>b,c</sup>	0.562 ± 0.072 <sup>b,c</sup>
<i>Gastrocnemius white (IIb)</i>		
Fc2	0.340 ± 0.081 <sup>a,c,d</sup>	0.272 ± 0.065 <sup>a,c</sup>
Fc0	0.660 ± 0.081 <sup>a,c,d</sup>	0.728 ± 0.065 <sup>a,c</sup>
<i>Soleus (I)</i>		
Fc2	0.565 ± 0.089 <sup>a,b,e</sup>	0.564 ± 0.096 <sup>a,b</sup>
Fc0	0.435 ± 0.089 <sup>a,b,e</sup>	0.436 ± 0.096 <sup>a,b</sup>
<i>Heart</i>		
Fc2	0.563 ± 0.066 <sup>b,e</sup>	
Fc0	0.437 ± 0.066 <sup>b,e</sup>	
<i>Liver</i>		
Fc2	0.367 ± 0.054 <sup>c,d</sup>	
Fc0	0.633 ± 0.054 <sup>c,d</sup>	

Results are means ± SD (*n* = 5). Fc2, fractional contribution from [2,4,6,8-<sup>13</sup>C<sub>4</sub>]octanoate; Fc0, contribution from unlabeled endogenous substrates. <sup>a</sup>Significantly different from predominantly red gastrocnemius muscle in same condition (rested vs. contracted), <sup>b</sup>significantly different from white gastrocnemius muscle in same condition, <sup>c</sup>significantly different from soleus muscle in same condition (heart and liver were compared with rested muscle), <sup>d</sup>significantly different from heart, <sup>e</sup>significantly different from liver (all *P* ≤ 0.05).

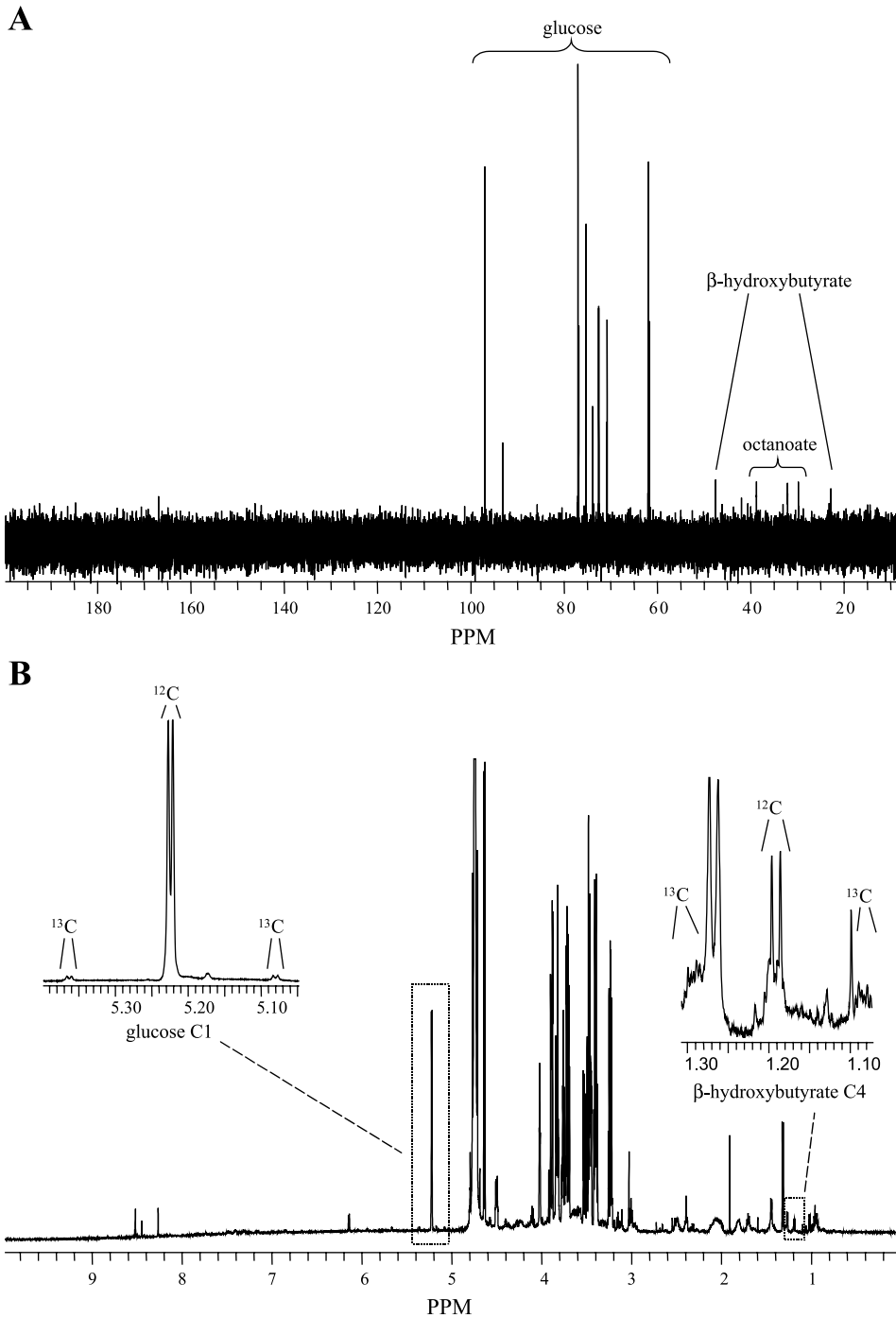


Fig. 3. Full <sup>13</sup>C (A) and <sup>1</sup>H (B) spectra from a representative extract of blood taken at the end of the experiment. In the <sup>13</sup>C spectrum, peaks are visible in the regions where carbons from glucose, [2,4,6,8-<sup>13</sup>C<sub>4</sub>]octanoate, and β-hydroxybutyrate resonate. Resonances from numerous metabolites are visible in the <sup>1</sup>H spectrum, with peaks arising from protons attached to unlabeled (<sup>12</sup>C) and labeled (<sup>13</sup>C) carbons. Glucose C-1 and β-hydroxybutyrate C-4 regions are expanded to show protons attached to the unlabeled carbon as well as those giving rise to the <sup>13</sup>C side peaks.

of the experiment after 60 min of infusion with [2,4,6,8-<sup>13</sup>C<sub>4</sub>]octanoate, indicating nearly 100% enrichment of blood octanoate.

#### DISCUSSION

Results from this study illustrate the utility of <sup>13</sup>C methodology in assessing octanoate oxidation within multiple tissues in an intact animal. We found that octanoate is a major contributor to the acetyl-CoA pool in all tissues examined, with the highest oxidation occurring in heart and soleus muscle, followed

by the predominantly red portion of the gastrocnemius muscle, with lower levels in liver and in the white portion of the gastrocnemius muscle (Table 2). These results are consistent with the hypothesis that the fractional contribution of octanoate to oxidative metabolism is a function of the oxidative capacity of the tissue. No differences were observed between rest and contraction in the fractional contribution of <sup>13</sup>C-labeled octanoate to the oxidative metabolism of either gastrocnemius or soleus muscles (Table 2), indicating that octanoate metabolism increases in

Table 3. *Physiological data*

	Endogenous	0 min	60 min
Glucose, mM	11.4 ± 1.7	12.0 ± 1.7	12.9 ± 2.0*
Pyruvate, μM	81.9 ± 26.5	78.3 ± 8.9	78.6 ± 12.4
Lactate, μM	273 ± 27	357 ± 46*	424 ± 66*
Ketones, μM	131 ± 78	362 ± 206*	423 ± 120*
FFA, μEq/l	62 ± 50	279 ± 169*	359 ± 117*
Octanoate, μM	N.D.	188 ± 33*	168 ± 38*
Insulin, ng/ml	0.20 ± 0.04	0.43 ± 0.24	1.60 ± 1.34

Results are means ± SD ( $n = 5$  except octanoate concentration for the 0 time point, where  $n = 4$  because of technical difficulties with 1 of the samples). Concentrations are shown before any octanoate infusion (endogenous), after the infusion of unlabeled octanoate but before infusion of <sup>13</sup>C-labeled octanoate (0 min), and at the end of the experiment (60 min). Ketones, β-hydroxybutyrate + acetoacetate; FFA, free fatty acids. Endogenous levels of octanoate were too low to be accurately measured (not detected, N.D.). \*Significantly different from endogenous ( $P \leq 0.05$ ).

contracted muscle proportionally to the overall increase in oxidative rate.

Non-steady-state analysis values of acetyl-CoA fractional enrichment from [2,4,6,8-<sup>13</sup>C<sub>4</sub>]octanoate in the heart and liver in these experiments (Table 2) correlated well with previously reported values calculated by steady-state analysis (20) in these tissues after infusion of a combination of [2,4,6,8-<sup>13</sup>C<sub>4</sub>]octanoate and [1,2,3,4-<sup>13</sup>C<sub>4</sub>]octanoate in the intact rat (9). Previous studies in heart (19) and liver (16) demonstrated that flux through anaplerotic pathways relative to TCA cycle flux is much higher in liver than heart. Additionally, pyruvate recycling may occur in liver (15). Flux of unlabeled substrates through anaplerotic pathways dilutes <sup>13</sup>C label in TCA cycle intermediates and is likely a contributor to the lower amount of label found in C-4 and C-3 multiplets in liver vs. heart. Moreover, high oxygen consumption and TCA cycle turnover combined with a large fraction of labeled acetyl-CoA generates elevated levels of labeled multiplets. This, combined with lower anaplerotic flux of unlabeled substrates, contributes to the dramatic increases found in multiplet label distribution in heart vs. liver (Fig. 2).

In muscle, the fractional contribution of <sup>13</sup>C-labeled octanoate was highest in soleus, followed by the predominantly red portion of the gastrocnemius muscle, and lowest in white gastrocnemius muscle (Table 2). An earlier study reported glutamate C-4 fractional enrichments in rested soleus and entire gastrocnemius muscles to be 0.60 and 0.66, respectively, after infusion with [2,4,6,8-<sup>13</sup>C<sub>4</sub>]octanoate and unlabeled lactate in the intact rat (14). This is similar to the non-steady-state fractional enrichment of predominantly red gastrocnemius and soleus muscle (Table 2) but substantially higher than the white portion of the gastrocnemius muscle (Table 2). This is explained by the markedly lower oxidative metabolism in the white portion of the gastrocnemius muscle than in the red portion (6).

*Isotopic steady state: implications from octanoate metabolism.* Although previous studies indicate that heart and liver are at isotopic steady state (ISS) after

60 min of <sup>13</sup>C-labeled octanoate infusion (9), it is unlikely that rested skeletal muscle achieves ISS by this time, given previous results with <sup>13</sup>C-labeled acetate (17, 25, 35). Lack of ISS is further supported by high glutamate C-4-to-C-3 resonance ratios in both rested and contracted soleus and gastrocnemius muscle (Table 1; Ref. 21). If mixing occurs at symmetrical TCA cycle intermediates and there is no contribution of anaplerotic flux of unlabeled substrates into the TCA cycle, C-4/C-3 will approach 1 at ISS. Lower C-3 enrichment, however, may also be due to the contribution of anaplerotic flux of unlabeled substrates into the TCA cycle (18, 19). This would also contribute to decreased signal in other multiplet regions of glutamate (e.g., the D34 in the glutamate C-4 region). Therefore, differences in flux through anaplerotic pathways may be partly responsible for the minor variations in label pattern among the distinct muscle fiber types. The same may be true of the substantial label pattern variations when muscle is compared with heart, although tissue differences in oxygen consumption, particularly for muscles at rest, are influential as well. Steady-state analysis including a longer time span will be necessary before ISS is confirmed and anaplerotic flux can be determined in muscle.

*Octanoate oxidation during muscle contraction.* Fractional contribution from octanoate to oxidative metabolism in contracted muscle ranged from 27% to 56% (Table 2). This is similar to the 49–55% contribution of fats to oxidative metabolism in human vastus lateralis muscle during rest and after 30 min of exercise at moderate intensity (up to 55% of maximum workload; Ref. 37). Relative (fractional) contribution of <sup>13</sup>C-labeled octanoate to the acetyl-CoA pool during contraction is not different from that during rest (Table 2), indicating an increase in octanoate metabolism that is proportional to the overall increase in oxidative rate.

*Other <sup>13</sup>C-labeled and unlabeled metabolites.* Plasma octanoate concentrations achieved in this study (Table 3) were similar to levels typically found in patients receiving MCT diets (4, 22). Thus pathophysiological substrate changes that can result after high doses of plasma octanoate (39) were eliminated. Free fatty acid concentration increased similarly to the increase in plasma octanoate levels (Table 3), and, although glucose and lactate levels were significantly different (Table 3), these increases were not substantial and were likely attributable to liver glycogenolysis and muscle lactate production that typically occurs during contraction. Liver ketogenesis was expected on the administration of octanoate, and blood ketone levels increased approximately threefold by the end of the experiment to 423 μM (Table 3), a value only slightly higher than those typically found in fed rats (29).

Examination of <sup>1</sup>H and <sup>13</sup>C spectra of blood extracts taken at the end of the experiments revealed that glucose and β-hydroxybutyrate were enriched above natural abundance levels (Fig. 3), most likely because of liver gluconeogenesis and ketogenesis, respectively. If significant oxidation of <sup>13</sup>C-labeled glucose had occurred in any of the tissues examined, it would be

manifested in contributions not only to the acetyl-CoA pool labeled in C-2 (Fc2) but also in C-1 (Fc1) and, to a lesser extent, in both carbons (Fc12). There was no evidence of <sup>13</sup>C-labeled glucose oxidation. Liver ketogenesis from [2,4,6,8-<sup>13</sup>C<sub>4</sub>]octanoate gives rise to ketones labeled in the C-2 and C-4 positions. However, the contribution of <sup>13</sup>C-labeled ketones to Fc2 would be indistinguishable from oxidation of [2,4,6,8-<sup>13</sup>C<sub>4</sub>]octanoate and could lead to an overestimation of octanoate oxidation. No unlabeled octanoate was detected at the end of the experiment (after 60 min of infusion with [2,4,6,8-<sup>13</sup>C<sub>4</sub>]octanoate), indicating that the enrichment of octanoate was virtually 100%. In contrast, β-hydroxybutyrate was found to be enriched 13.5%. Although some label contribution to Fc2 may have been from ketones, our study does not permit a precise determination of this amount. However, ketone contribution to Fc2 (Fc2<sub>ket</sub>) can be estimated with previously reported ketone utilization values (U<sub>ket</sub>) in the fed state (1, 12, 28): Fc2<sub>ket</sub> = 0.135 × U<sub>ket</sub>. Utilization values are expressed as a percentage of total substrate use. Octanoate contribution to Fc2 can be adjusted with the equation Fc2<sub>oct</sub> = Fc2 - Fc2<sub>ket</sub>. Because octanoate <sup>13</sup>C-enrichment was 100% in our experiments, Fc2<sub>oct</sub> = U<sub>oct</sub>. With a physiological substrate mix found in the blood of normal fed rats containing fatty acids, lactate, glucose, and acetoacetate, ketone usage was calculated to be 23% in heart, with fatty acids and lactate comprising the remainder of oxidative metabolism (12). If this level of utilization occurred in our experiments, <sup>13</sup>C-enriched ketone contribution to Fc2 in heart was 0.03 (0.135 × 0.23), with octanoate contributing 0.533 (0.563 - 0.03) to oxidative metabolism. In the livers of fed rats, acetoacetate and β-hydroxybutyrate are released into the blood whereas fatty acids, lactate, and alanine are removed from the blood (28). Given the ketogenic nature of liver, especially in the presence of octanoate, it is improbable that liver is oxidizing <sup>13</sup>C-labeled ketones from the blood and contributing to observed Fc2 values in that tissue (Table 2). Carbohydrates and fats are the primary substrates used in the fed condition by skeletal muscle (11, 31). In the isolated, perfused hindquarter of fed rats, ketone oxidation was negligible in rested skeletal muscle with perfusion concentrations of 3.4 mM ketones and was not different after a bout of strenuous exercise (1). In that same study, a longer, less strenuous exercise protocol and perfusion ketone concentrations of 10 mM resulted in an almost twofold increase in skeletal muscle ketone body utilization (1). Because we used a moderate intensity contraction protocol and blood ketone levels were well under 1 mM (Table 3), it is unlikely that there was a significant <sup>13</sup>C-enriched ketone contribution to Fc2 in either resting or contracted skeletal muscle. Thus, although <sup>13</sup>C-labeled ketones may have contributed to oxidative metabolism, contribution to Fc2 (0.0–0.03) is small relative to that of octanoate in all tissues examined (0.272–0.565; Table 2).

In conclusion, we found that [2,4,6,8-<sup>13</sup>C<sub>4</sub>]octanoate contributes >50% of the acetyl-CoA pool in heart and

soleus muscle, ~45% in predominantly red gastrocnemius muscle, and ~30% in liver and white gastrocnemius muscle under normal physiological conditions. During muscle contraction, the proportion of octanoate contribution to acetyl-CoA production remains high. Our findings demonstrate that the fractional contribution of octanoate to oxidative metabolism correlates with the oxidative capacity of the tissue and that octanoate metabolism increases in contracted muscle proportionally to the overall increase in oxidative rate.

The authors gratefully acknowledge the laboratory of Dr. Henri Brunengraber for plasma octanoate concentration and enrichment measurements and Kay McCorkle for assistance with insulin assays. We also thank Dr. Craig Malloy for constructive conversations regarding this work.

## DISCLOSURES

This study was supported by an Associate Investigator award and Merit (no. 98-139) and Veterans Integrated Service Network 17 (no. 99-89) grants from the Department of Veterans Affairs.

## REFERENCES

- Berger M, Kemmer FW, Goodman MN, Zimmermann-Telschow H, and Ruderman NB. Ketone body metabolism in isolated perfused muscle in various metabolic states. In: *Biochemical and Clinical Aspects of Ketone Body Metabolism*, edited by Söling H-D and Seufert C-D. Littleton, MA: PSG Publishing, 1978, p. 193–203.
- Carnielli VP, Sulkers EJ, Moretti C, Wattimena JLD, van Goudoever JB, Degenhart HJ, Zachello F, and Sauer PJJ. Conversion of octanoic acid into long-chain saturated fatty acids in premature infants fed a formula containing medium-chain triglycerides. *Metabolism* 43: 1287–1292, 1994.
- Coyle EF, Jeukendrup AE, Wagenmakers AJM, and Saris WHM. Fatty acid oxidation is directly regulated by carbohydrate metabolism during exercise. *Am J Physiol Endocrinol Metab* 273: E268–E275, 1997.
- Dean HG, Bonser JC, and Gent JP. HPLC analysis of brain and plasma for octanoic and decanoic acids. *Clin Chem* 359: 1945–1948, 1989.
- Décombaz J, Arnaud MJ, Milon H, Moesch H, Philipposian G, Thélain AI, and Howald H. Energy metabolism of medium-chain triglycerides versus carbohydrates during exercise. *Eur J Appl Physiol* 52: 9–14, 1983.
- De Ruiter J, De Haan A, and Sargeant AJ. Physiological characteristics of two extreme muscle compartments in gastrocnemius medialis of the anaesthetized rat. *Acta Physiol Scand* 153: 313–324, 1995.
- Dyck DJ, Peters SJ, Glatz J, Gorski J, Keizer H, Kiens B, Liu S, Richter EA, Spriet LL, van der Vusse GJ, and Bonen A. Functional differences in lipid metabolism in resting skeletal muscle of various fiber types. *Am J Physiol Endocrinol Metab* 272: E340–E351, 1997.
- From AHL, Zimmer SD, Michurski SP, Mahonakrishnan P, Ulstad VK, Thoma WJ, and Ugurbil K. Regulation of the oxidative phosphorylation rate in the intact cell. *Biochemistry* 29: 3731–3743, 1990.
- Gavva SR, Wiethoff AJ, Zhao P, Malloy CR, and Sherry AD. A <sup>13</sup>C isotopomer n.m.r. method for monitoring incomplete β-oxidation of fatty acids in intact tissue. *Biochem J* 303: 847–853, 1994.
- Gillingham M, Van Calcar S, Ney D, Wolff J, and Harding C. Dietary management of long-chain 3-hydroxyacyl-CoA dehydrogenase deficiency (LCHADD). A case report and survey. *J Inher Metab Dis* 22: 123–131, 1999.
- Gollnick PD and Saltin B. *Fuel for Muscular Exercise: Role of Fat*. New York: Macmillan, 1988.
- Jeffrey FMH, Diczku V, Sherry AD, and Malloy CR. Substrate selection in the isolated working rat heart: effects of

- reperfusion, afterload, and concentration. *Basic Res Cardiol* 90: 388–396, 1995.
13. **Jeukendrup AE, Saris WHM, Van Diesen R, Brouns F, and Wagenmakers AJM.** Effect of endogenous carbohydrate availability on oral medium-chain triglyceride oxidation during prolonged exercise. *J Appl Physiol* 80: 949–954, 1996.
  14. **Jones JG, Hansen J, Sherry AD, Malloy CR, and Victor RG.** Determination of acetyl-CoA enrichment in rat heart and skeletal muscle by <sup>1</sup>H nuclear magnetic resonance analysis of glutamate in tissue extracts. *Anal Biochem* 249: 201–206, 1997.
  15. **Jones JG, Naidoo R, Sherry AD, Jeffrey FMH, Cottam GL, and Malloy CR.** Measurement of gluconeogenesis and pyruvate recycling in the rat liver: a simple analysis of glucose and glutamate isotopomers during metabolism of [1,2,3-<sup>13</sup>C]propionate. *FEBS Lett* 412: 131–137, 1997.
  16. **Jucker BM, Lee JY, and Shulman RG.** In vivo <sup>13</sup>C NMR measurements of hepatocellular tricarboxylic acid cycle flux. *J Biol Chem* 273: 12187–12194, 1998.
  17. **Jucker BM, Rennings AJM, Cline GW, Petersen KF, and Shulman GL.** In vivo NMR investigation of intramuscular glucose metabolism in conscious rats. *Am J Physiol Endocrinol Metab* 273: E139–E148, 1997.
  18. **Malloy CR, Sherry AD, and Jeffrey FMH.** Carbon flux through citric acid cycle pathways in perfused heart by <sup>13</sup>C NMR spectroscopy. *FEBS Lett* 212: 58–62, 1987.
  19. **Malloy CR, Sherry AD, and Jeffrey FMH.** Evaluation of carbon flux and substrate selection through alternate pathways involving the citric acid cycle of the heart by <sup>13</sup>C NMR spectroscopy. *J Biol Chem* 263: 6964–6971, 1988.
  20. **Malloy CR, Sherry AD, and Jeffrey FMH.** Analysis of tricarboxylic acid cycle of the heart using <sup>13</sup>C isotope isomers. *Am J Physiol Heart Circ Physiol* 259: H987–H995, 1990.
  21. **Malloy CR, Thompson JR, Jeffrey FMH, and Sherry AD.** Contribution of exogenous substrates to acetyl coenzyme A: measurement by <sup>13</sup>C NMR under non-steady-state conditions. *Biochemistry* 29: 6756–6761, 1990.
  22. **Mascioli EA, Lopes S, Randall S, Porter KA, Kater G, Hirschberg Y, Babayan VK, Bistrain BR, and Blackburn GL.** Serum fatty acid profiles after intravenous medium chain triglyceride administration. *Lipids* 24: 793–798, 1989.
  23. **Maughan RJ.** A simple, rapid method for the determination of glucose, lactate, pyruvate, alanine, 3-hydroxybutyrate and acetoacetate on a single 20- $\mu$ l blood sample. *Clin Chim Acta* 122: 231–240, 1982.
  24. **McGarry JD and Foster DW.** The metabolism of (–)octanoyl-carnitine in perfused livers from fed and fasted rats. Evidence for a possible regulatory role of carnitine acyltransferase in the control of ketogenesis. *J Biol Chem* 249: 7984–7990, 1974.
  25. **Mezzarobba V, Bielicki G, Jeffrey FMH, Mignon M, Renou JP, Grizard J, and Meynial-Denis D.** Lack of effect of ageing on acetate oxidation by rat skeletal muscle during starvation: a <sup>13</sup>C NMR study. *J Exp Biol* 203: 995–1001, 2000.
  26. **Powers L, Osborn MK, Kien CL, Murray RD, M, and Brunengraber H.** Assay of the concentration and stable isotope enrichment of short-chain fatty acids by gas chromatography-mass spectrometry. *J Mass Spectrom* 30: 747–754, 1995.
  27. **Rasmussen BB and Wolfe RR.** Regulation of fatty acid oxidation in skeletal muscle. *Annu Rev Nutr* 19: 463–484, 1999.
  28. **Rémésy C and Demigné C.** Changes in availability of glucogenic and ketogenic substrates and liver metabolism in fed or starved rats. *Ann Nutr Metab* 27: 57–70, 1983.
  29. **Robinson AM and Williamson DH.** Physiological roles of ketone bodies as substrates and signals in mammalian tissues. *Physiol Rev* 60: 143–187, 1980.
  30. **Rouis M, Dugi KA, Previato L, Patterson AP, Brunzell JD, Brewer HB, and Santamarina-Fojo S.** Therapeutic response to medium-chain triglycerides and  $\omega$ -3 fatty acids in a patient with the familial chylomicronemia syndrome. *Arterioscler Thromb Vasc Biol* 17: 1400–1406, 1997.
  31. **Saltin B and Gollnick PD.** *Fuel for Muscular Exercise: Role of Carbohydrate.* New York: Macmillan, 1988.
  32. **Sidossis LS, Gastaldelli A, Klein S, and Wolfe RR.** Regulation of plasma fatty acid oxidation during low- and high-intensity exercise. *Am J Physiol Endocrinol Metab* 272: E1065–E1070, 1997.
  33. **Sidossis LS, Wolfe RR, and Coggan AR.** Regulation of fatty acid oxidation in untrained versus trained men during exercise. *Am J Physiol Endocrinol Metab* 274: E510–E515, 1998.
  34. **Sulkers EJ, Lafeber HN, and Sauer PJJ.** Quantitation of oxidation of medium-chain triglycerides in preterm infants. *Pediatr Res* 26: 294–297, 1989.
  35. **Szczepaniak L, Babcock EE, Malloy CR, and Sherry AD.** Oxidation of acetate in rabbit skeletal muscle: detection by <sup>13</sup>C NMR spectroscopy in vivo. *Magn Reson Med* 36: 451–457, 1996.
  36. **Taegtmeier H, Hems R, and Krebs HA.** Utilization of energy-providing substrates in the isolated working rat heart. *Biochem J* 186: 701–711, 1980.
  37. **Van Loon LJ, Greenhaff PL, Constantin-Teodosiu D, Saris WH, and Wagenmakers AJ.** The effects of increasing exercise intensity on muscle fuel utilisation in humans. *J Physiol* 536: 295–304, 2001.
  38. **Wagenmakers AJM and Veerkamp JH.** Interaction of octanoate with branched-chain 2-oxo acid oxidation in rat and human muscle in vitro. *Int J Biochem* 16: 977–984, 1984.
  39. **Yeh Y-Y and Zee P.** Relation of ketosis to metabolic changes induced by acute medium-chain triglyceride feeding in rats. *J Nutr* 106: 58–67, 1976.